

## PCILO quantum-mechanical relaxed conformational energy map of methyl 4-thio- $\alpha$ -maltoside in solution

Karim Mazeau

*Centre de Recherches sur les Macromolécules Végétales, B.P. 53 X, 38041 Grenoble (France)*

and Igor Tvaroska

*Institute of Chemistry, Slovak Academy of Sciences, 84238 Bratislava (Czechoslovakia)*

(Received November 2nd, 1990; accepted in revised form September 19th, 1991)

### ABSTRACT

A theoretical study is presented of the conformational properties of methyl 4-thio- $\alpha$ -maltoside. Quantum-chemical PCILO (perturbed configuration interaction with localized orbitals) energy minimization with evaluation of the solvent effect has been used to calculate semi-rigid and relaxed ( $\Phi$ ,  $\Psi$ ) conformational-energy surfaces in 1,4-dioxane, methanol, dimethyl sulfoxide, and water. The inclusion of molecular flexibility in the conformational analysis of this disaccharide derivative was found to have a significant effect upon the allowed conformational space of the molecule. Calculations revealed the existence of 15 stable conformers having different internal geometries. The relative abundance of these conformers is strongly influenced by solvent. The locations of the global minima and “virtual” conformations vary with solvent and the flexibility of methyl 4-thio- $\alpha$ -maltoside significantly decreases from 1,4-dioxane to water. It was found that the conformational properties of methyl 4-thio- $\alpha$ -maltoside differ from those of the corresponding 4-oxygenated analogue, methyl  $\alpha$ -maltoside. The calculated solution behaviour is supported by very good agreement between the theoretical values  $\langle {}^3J_{C4,H-1'} \rangle = 2.67$  and  $\langle {}^3J_{C-1',H-4} \rangle = 5.24$  Hz calculated as ensemble averages over all conformers on the relaxed map and the experimental values of 2.95 and 5.15 Hz in water solution.

### INTRODUCTION

Thio sugars frequently act as inhibitors of enzymes for which the corresponding non-sulphur saccharide is a substrate. For example, 1-thiooligosaccharides are good substrate analogues for studies of glycanases<sup>1</sup>. Replacement of oxygen by sulphur modifies the geometry of the molecules and may alter conformational behaviour around the glycosidic linkage. The three-dimensional structure of a substrate in solution is one of the factors that controls enzyme–substrate interactions. Therefore, investigation of the conformational properties of 1-thiooligosaccharides is of interest.

One crystal structure for a thio-oligosaccharide, methyl 4-thio- $\alpha$ -maltoside, has been reported<sup>2</sup>. The torsional angles  $\Phi = O-5'-C-1'-S-C-4$  and  $\Psi = C-1'-S-C-4-C-5$  of the glycosidic linkage in the crystal structure of this compound are 89 and  $-116.8^\circ$ , respectively. Recently, interglycosidic carbon–proton coupling constants of  ${}^3J_{C-1',H-4}$  5.15 and  ${}^3J_{C4,H-1'}$  2.95 Hz were measured for methyl 4-thio- $\alpha$ -maltoside in water solution in connection with a determination of the Karplus-type relationship for thio sugars<sup>3</sup>.

Conformational-energy calculations<sup>2</sup> using a simple method, treating only non-bonded interaction and torsion-potential terms with the barrier of 2.1 kJ/mol about the C–S bond estimated from PCILO (perturbed configuration interaction with localized orbitals) calculations<sup>4</sup> of acyclic model compounds, showed that the overall shape of the ( $\Phi$ ,  $\Psi$ ) map is similar to that calculated for maltose, and the minimum-energy conformation was found at  $\Phi = 45^\circ$  and  $\Psi = -160^\circ$ .

A number of problems complicate the use of conformational analysis for understanding three-dimensional structures (that is, conformational properties) of thiooligosaccharides. For example, it is now well recognized<sup>5</sup> that, as a disaccharide molecule undergoes rotation about the glycosidic torsional angles; the pyranoid rings are not rigid. Because of changes in the internal coordinates, such as bond lengths, bond angles, ring torsional angles, and pendant-group orientations, a more-realistic approximation is given by calculation of a relaxed (or adiabatic) conformational-energy map. However, the potential-energy functions in molecular-mechanics programs cannot accommodate the thioacetal sequences of atoms occurring in 1-thiooligosaccharides. Therefore, to understand the conformational properties of 1-thiooligosaccharides it is necessary to perform calculations using reliable quantum mechanical methods. In this paper we report the calculation of a relaxed conformational-energy map for methyl 4-thio-maltoside in several solvents. These results are the first quantum-mechanical relaxed maps to be reported for a disaccharide system.

#### METHODS OF CALCULATION

**Nomenclature.** — A schematic representation of methyl 4-*S*- $\alpha$ -D-glucopyranosyl-4-thio- $\alpha$ -D-glucopyranoside (methyl 4-thio- $\alpha$ -maltoside, **1**) and its numbering\* is shown in Fig. 1. The notation of the individual conformers is based on the values of torsional angles  $\Phi$  [O-5'-C-1'-S-C-4] and  $\Psi$  [C-1'-S-C-4-C-3] that describe the relative orientation of the glucopyranose residues. For calculations of the C–H coupling constants, the torsional angles  $\Phi^H$  [H-1'-C-1'-S-C-4] and  $\Psi^H$  [C-1'-S-C-4-H-4] with the reference to the hydrogen atoms are used. The orientation of the primary hydroxyl group in the glucose rings is defined by a torsional angle  $\omega$  [O-5'-C-5'-C-6'-O-6'] and the three staggered conformations of the glucose hydroxymethyl group  $\omega = 60, 180$ , and  $-60^\circ$  correspond to the *gauche-trans* (*gt*), *trans-gauche* (*tg*) and *gauche-gauche* (*gg*) orientations. Interglycosidic proton–proton distances are described as  $r_{ij}$ , thus  $r_{14}$  refers to distance between the H-1' and H-4 protons. The internal geometry is based on the crystal-structure geometry of methyl 4-thio- $\alpha$ -maltoside<sup>2</sup>. The coordinates of the hydrogen atoms were determined by using a C–H bond length of 110 pm, and an O–H bond lengths of 99 pm, with a bond vector related appropriately to the C–C and C–O bond vectors.

\* Following conventional practice, the atoms of the methyl 4-thio-glycoside residue are unprimed and those of the  $\alpha$ -D-glucopyranosyl group are primed.

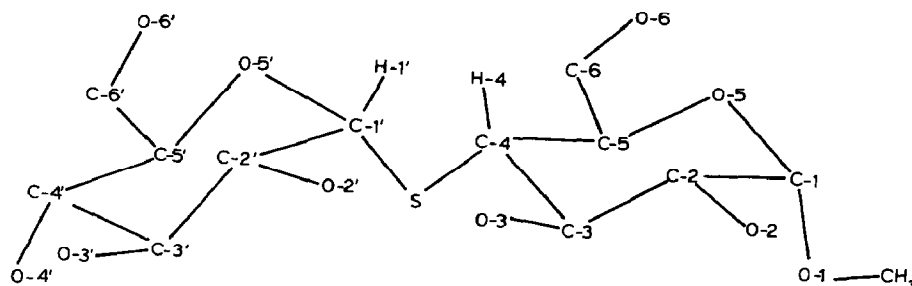


Fig. 1. Schematic representation of the methyl 4-thio- $\alpha$ -maltoside molecule, indicating the labeling of the atoms. For simplicity, all of the hydrogen atoms except H-1 and H-4 are omitted.

**Quantum-mechanical calculations.** — The energy of each conformer was calculated by using the quantum-mechanical PCILO method<sup>6</sup>. We selected this method as it has been successful in predicting the conformational properties of saccharides, and the results on model compounds for the thioglycosidic linkage are comparable with those obtained by *ab initio* calculations<sup>4,7</sup>. Calculation of the solvent influence on conformer stability in dilute solution has been described in detail in our previous papers<sup>8,9</sup>. Despite the approximations used in the terms of the reaction-field model of solvent-effect calculations, this method has been successfully applied to the study of carbohydrate conformations in different solutions<sup>10</sup>. The conformational properties of methyl 4-thio- $\alpha$ -maltoside are expressed in forms of semi-rigid and relaxed two-dimensional conformational ( $\Phi$ ,  $\Psi$ ) maps.

**Semi-rigid ( $\Phi$ ,  $\Psi$ ) maps.** — A semi-rigid map was prepared by rotating the rigid residue from the crystal geometry of 1 to each combination of  $\Phi$  and  $\Psi$  on the  $10^\circ$  grid and evaluating the PCILO energy. There are also 9 possible combinations of staggered orientations for the hydroxymethyl groups in methyl 4-thio- $\alpha$ -maltoside. It has been shown<sup>11</sup> that the orientations of these groups influence the shape of the ( $\Phi$ ,  $\Psi$ ) map for maltose. Therefore, for each ( $\Phi$ ,  $\Psi$ ) point, the best of the nine different orientations of the two hydroxymethyl groups, was used. Subsequently, the solvation-energy maps for four solvents, namely 1,4-dioxane, methanol, dimethyl sulfoxide, and water were calculated and superimposed on the PCILO ( $\Phi$ ,  $\Psi$ ) map to give solvent-specific, semi-rigid ( $\Phi$ ,  $\Psi$ ) maps.

**Relaxed ( $\Phi$ ,  $\Psi$ ) maps.** — In order to examine the influence of internal flexibility on the available conformational space, a relaxed map of methyl 4-thio- $\alpha$ -maltoside was produced by allowing the 81 molecular geometry parameters to relax to give the lowest-energy conformation corresponding to each combination of glycosidic angles. To prepare this map, points were selected at regular  $30^\circ$  intervals on the semi-rigid ( $\Phi$ ,  $\Psi$ ) map. The energies of all the conformers were minimized by the non-derivative method of conjugate directions with the Powell-Zangwill algorithm<sup>12,13</sup> in the space of the internal coordinates. The accuracy of the optimized geometrical parameters was 0.1 pm for bond lengths,  $0.01^\circ$  for bond angles, and  $0.1^\circ$  for torsional angles. The positions of the minima on the relaxed ( $\Phi$ ,  $\Psi$ ) map were refined by relaxing the torsional angles  $\Phi$

and  $\Psi$ . Subsequently, solvent-specific, relaxed conformational ( $\Phi$ ,  $\Psi$ ) maps were obtained by the same approach as used for semi-rigid maps.

*Ensemble-averages.* — Statistical mechanics was utilized to calculate ensemble average molecular characteristics from the relaxed map where the torsional angles  $\Phi$  and  $\Psi$  served to approximate the overall surface. The relative population of the  $i,j$ -th conformational microstate,  $x_{ij}$ , is governed by the Boltzmann distribution such that:

$$x_{ij} = \exp [-G_{ij}(\Phi, \Psi)/RT]/Q \quad (1)$$

where  $Q$ , the classical partition function, is given by

$$Q = \sum_i \sum_j \exp[-\Delta G_{ij}(\Phi, \Psi)/RT] \quad (2)$$

Any molecular parameter,  $P_{ij}$ , may be calculated for each conformational microstate and the ensemble average parameter  $\langle P \rangle$  is then defined as:

$$\langle P \rangle = \sum_i \sum_j P_{ij} \quad (3)$$

It was of particular interest to compare these ensemble averages which define "virtual" conformation with the subset of solution conformations found on the relaxed maps.

*Coupling constants.* — Interresidue coupling constants  $^3J_{C,H}$  were calculated by using a recently proposed<sup>3</sup> angular dependence of the carbon-proton coupling constant for C-S-C-H segments:

$$^3J_{C,H} = 4.44\cos^2\varphi^H - 1.06\cos\varphi^H + 0.45 \quad (4)$$

Ensemble average coupling constants were then calculated by using Eq. 3.

All calculations were carried out on the IRIS computer at CERMAV, and the calculation of each point on the relaxed map of **1** required 7 h of CPU time. Molecular drawings were produced by using software from Polygen Corp. Quanta, Version 3.0.

## RESULTS AND DISCUSSION

*Semi-rigid ( $\Phi$ ,  $\Psi$ ) maps.* — Fig. 2 shows the semi-rigid conformational ( $\Phi$ ,  $\Psi$ ) maps for an isolated methyl 4-thio- $\alpha$ -maltoside molecule (Fig. 2a) and its aqueous solution (Fig. 2b). The semi-rigid maps may be divided into two parts, north and south by the  $\Psi$  coordinate at  $\sim 150^\circ$ . Inspection of the vacuum ( $\Phi$ ,  $\Psi$ ) map revealed the existence of six minima. In the north part, four calculated minima are found and the lowest-energy minimum lies at  $\Phi = 45^\circ$  and  $\Psi = -165^\circ$ . The lowest local minimum in the south part is located at  $(60^\circ, 60^\circ)$  with an energy  $\sim 3$  kJ/mol higher than that of the global minimum. The crystallographic conformation<sup>2</sup> ( $89^\circ, -116.8^\circ$ ) of **1** is close to one of the local minima in the north part ( $90^\circ, -105^\circ$ ) with an energy 6 kJ/mol relative to the main minimum. The north and south parts of the semi-rigid vacuum map are enclosed

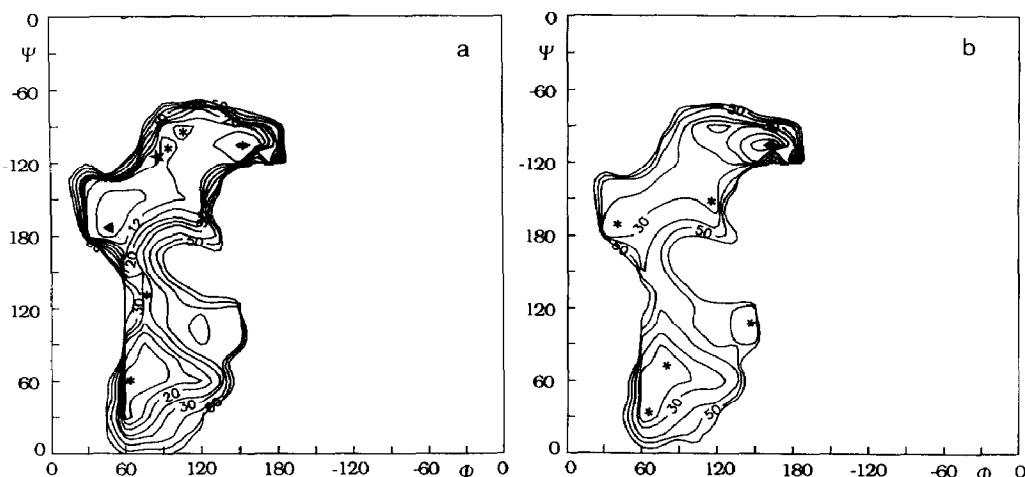


Fig. 2. Semi-rigid PCILO energy surface (kJ/mol) for methyl 4-thio- $\alpha$ -maltoside [(a) isolated molecule, and (b) aqueous solution]. Contours are at 8, 12, 16, 20, 25, 30, 40, 50, and 60 kJ/mol above the energy minimum. The  $\Phi$ ,  $\Psi$  locations of the lowest minimum is indicated by  $\blacktriangle$ , and \* indicates local minima. The crystal structure is indicated by  $\star$ .

by the 30 kJ/mol contour. A conformational transition from the north region to south requires passage through a narrow valley with a barrier of  $\sim 25$  kJ/mol, whereas, in the potential-function map, the north and south regions are clearly separated by a barrier  $> 50$  kJ/mol. The barrier of the transition in the opposite direction is  $\sim 19$  kJ/mol. The overall shape of the vacuum map and the occurrence of the low-energy domains are similar to those calculated by simple potential functions<sup>2</sup>. This observation implies that the limits for the overall shape of the rigid map are defined mainly by contributions from steric interactions. The finer details (the relative energy of conformers) are determined by a proper evaluation of intermolecular interactions which include, for example, electrostatic interactions, the exo-anomeric effect, hydrogen bonding, and other factors.

A comparison of the semi-rigid maps for **1** in different solvents with that for an isolated methyl 4-thio- $\alpha$ -maltoside molecule shows that the main features of the vacuum map are preserved. However, significant alternations in the character of the maps inside the 50 kJ/mol contour may be observed as a result of the solvent effect. This is demonstrated in Fig. 2b for an aqueous solution, where the effect of solvent is most pronounced. Our results demonstrate that an increase of solvent polarity leads to a strong stabilization of the region around  $\Phi = 150^\circ$  in the north part of the map. Simultaneously, the barrier of the transition from the north to the south gradually increases up to 45 kJ/mol. Consequently, the principal conformer is located at  $(45^\circ, -165^\circ)$  in vacuum and 1,4-dioxane, whereas in methanol, dimethyl sulfoxide, and aqueous solution the principal conformer is predicted to be at  $(165^\circ, -105^\circ)$ . In aqueous solution, this latter conformer is also a major one. Interestingly, based on the semi-rigid map calculations for **1**, marked differences exist between solvent-induced conformational changes for methyl 4-thio- $\alpha$ -maltoside and those for its 4-oxygen

analogue maltose. In the case of maltose, the calculation suggests that, in aqueous solution, at least four conformers exist in equilibrium<sup>14</sup>.

*Vacuum-relaxed ( $\Phi$ ,  $\Psi$ ) map.* — The final vacuum PCILO relaxed potential ( $\Phi$ ,  $\Psi$ ) surface of **1** is shown in Fig. 3. This relaxed surface may be compared to the semi-rigid ( $\Phi$ ,  $\Psi$ ) vacuum map (Fig. 2a) produced by rigidly rotating the glucose residues to give the best orientation of the exocyclic hydroxymethyl groups. Although two low-energy domains, north and south, of the semi-rigid map may be identified on the relaxed map, the overall shapes of the two maps are completely different. This clearly shows how the constraints of rigid geometry limit the accessible conformations of **1**. In the semi-rigid map, steric interactions determine the general topology of the available space given by the 60 kJ/mol contour. It is evident that in the relaxed map this contour encompasses almost the whole ( $\Phi$ ,  $\Psi$ ) surface. This indicates a decrease importance of steric interactions. Interestingly, while the shape of the semi-rigid map of **1** is similar to rigid map of maltose, there are several important differences between the relaxed maps of methyl 4-thio- $\alpha$ -maltoside and maltose<sup>15,16</sup>. Perhaps the most significant of these is that the accessible space of **1** is considerably larger than that for maltose. Also, the global minimum of the relaxed map of **1**, T1, is not the lowest energy form on the MM2CARB map<sup>15</sup>, nor on the CHARMM map<sup>13</sup> where the conformers ( $60^\circ$ ,  $-140^\circ$ ) and ( $140^\circ$ ,  $-100^\circ$ ), respectively, are lower. Based on these differences, a different flexibility for both molecules may be expected. It has been shown that the exoanomeric effect in a thioacetal segment is lower than in a corresponding acetal segment<sup>7</sup>. This may be one of the reasons for the larger flexibility of **1** in comparison with maltose. Many other important features of ( $\Phi$ ,  $\Psi$ ) conformational space of **1** result from the relaxation

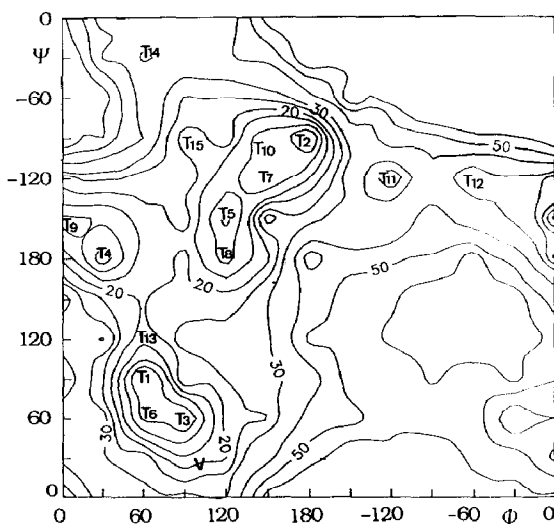


Fig. 3. Relaxed PCILO energy surface (kJ/mol) for methyl 4-thio- $\alpha$ -maltoside in a vacuum. Contours are at 8, 12, 16, 20, 25, 30, 40, 50, and 60 kJ/mol around the energy minimum. The  $\Phi$ ,  $\Psi$  locations of the minima T1, T2, T3, T4, T5, T6, T7, T8, T9, T10, T11, T12, T13, T14, and T15 and "virtual" conformation, V, are indicated.

TABLE I

Summary of the selected internal coordinates (bond distances (pm),  $r(1) = C-1'-S$ ,  $r(2) = S-C-4$ ; bond angles ( $^\circ$ ),  $\alpha = O-5'-C-1'-S$ ,  $\beta = C-1'-S-C-4$ ; torsion angles ( $^\circ$ ),  $\Phi$ ,  $\Psi$ ,  $\omega_1$ ,  $\omega_2$ ); proton-proton distances  $r_{14}$ ,  $r_{13}$  (pm), and dipole moment  $\mu$  (D) calculated for the 15 local minima of methyl 4-thio- $\alpha$ -maltoside by PCIO method compared with the corresponding crystal-structure values

Conformer	$\Phi$	$\Psi$	$\omega_1$	$\omega_2$	$\alpha$	$\tau$	$r(1)$	$r(2)$	$r_{14}$	$r_{13}$	$\mu$
T1	60.6	89.6	43.8	44.2	113.0	103.9	191.9	191.0	407.2	247.5	2.7
T2	179.9	-88.9	-54.5	-76.9	105.5	104.7	192.4	190.9	309.1	497.5	6.5
T3	90.1	59.5	-54.8	164.7	110.2	101.2	192.0	190.9	381.7	255.6	7.5
T4	31.7	179.4	-55.3	171.1	112.4	105.2	191.9	191.3	373.2	307.1	3.3
T5	119.8	-151.2	-54.2	170.1	108.9	98.7	192.2	191.1	207.6	381.0	5.7
T6	61.5	62.0	62.2	-65.4	108.9	101.2	191.9	191.2	397.3	289.8	3.4
T7	148.5	-119.8	-54.0	174.8	107.0	102.4	192.2	191.3	225.6	467.6	3.6
T8	121.3	-177.8	-53.5	176.2	108.0	101.4	192.5	190.9	253.2	336.9	5.6
T9	5.8	-152.7	-177.3	175.7	113.3	103.8	191.9	191.1	359.2	379.8	4.1
T10	143.9	-89.7	-53.9	-74.5	107.6	99.4	192.4	191.0	235.1	471.3	4.0
T11	-120.1	-120.0	-54.3	-164.8	107.9	107.7	192.2	191.1	368.6	519.4	4.9
T12	-62.3	-122.1	-175.1	-87.1	111.7	109.1	192.1	190.9	395.6	499.6	6.4
T13	59.8	119.6	-6.1	170.2	111.2	103.1	191.8	191.4	397.9	199.5	4.1
T14	63.8	-30.4	-55.2	34.5	111.5	108.6	191.7	191.1	314.4	484.8	5.6
T15	91.8	-89.6	-1.4	163.5	110.3	101.5	192.2	190.9	210.7	462.4	4.1
X-Ray	89.0	-116.8	62.0	-177.8	113.9	100.3	182.6	182.8			

of the geometrical parameters such as a lowering of energy barriers and the occurrence of the low-energy domain at  $\Phi \sim 30^\circ$  and  $\Psi \sim 180^\circ$ . This domain does not appear on the semi-rigid map, nor in any of the relaxed maps of maltose. The global minimum lies at  $(60^\circ, 90^\circ)$  and the preliminary recognition of the  $(\Phi, \Psi)$  map delineated 18 other conformers. As the map was calculated at regular  $30^\circ$  intervals on a grid in  $(\Phi, \Psi)$  space, it was necessary to characterize precisely all major conformations on the map. Therefore, several additional minimizations were carried out without the constraints on  $\Phi$  and  $\Psi$ .

*Structure of the stable conformers.* — Table I lists values for selected internal coordinates of the resulting 15 minima of methyl 4-thio- $\alpha$ -maltoside; values for glycosidic proton–proton distances and dipole moments are included. As may be seen, the conformers are located in three low-energy domains. Whereas for maltose, the torsional angle  $\Phi$  in the calculated minima<sup>15,16</sup> is in the range of  $60$ – $165^\circ$ , in the case of **1** it is distributed between  $5^\circ$  and  $-60^\circ$ . In six conformers of **1**, the angle  $\Phi$  is oriented in the *synclinal* (*sc*) position, five conformers have the *anticlinal* (*ac*) orientation, in two conformers the  $\Phi$  angle is in *synperiplanar* (*sp*) orientation and one conformer is in each of the *antiperiplanar* (*ap*), *-sc*, and *-ac* positions, respectively. Similarly, values of the angle  $\Psi$  may be clustered into five domains. Four conformers of **1** are in each of the *ap* and *-sc* orientations, respectively, three conformers have the  $\Phi$  in *sc* position, and two conformers are in each of the *ac*, and *-ac* orientations.

From Table I, it may be seen that orientations of the torsional angles  $\omega_i$  vary from conformer to conformer and the distribution of *gg*, *gt*, and *tg* conformers in minima is different for the reducing and for nonreducing residues. A straightforward application of Eq. 3 yields the following abundance of conformers in vacuum: *gg:gt:tg* = 51:48:1 for the  $\omega_1$  and *gg:gt:tg* = 27:45:28 for the  $\omega_2$  angles.

The distribution of optimized conformers in the direction of the angle  $\Phi$  is in accordance with a lower magnitude of the exoanomeric effect in thiooligosaccharides than in the *O*-glycosides. However, the manifestation of the exoanomeric effect in the thioacetal geometry can still be observed. The valence angles O-5'-C-1'-S and C-1'-S-C-4 are dependent on the orientation at the anomeric bonds. The O-5'-C-1'-S angle exhibits the largest variations that ranges from  $105.5$  to  $113.3^\circ$ ; the lowest value corresponds to the *ap* orientation of the angle  $\Phi$ . The calculated values of the glycosidic angle  $\tau[\text{C-1'-S-C-4}]$  are in the range  $98.7$ – $109.1^\circ$ . Carbon–sulphur bond lengths vary as a function of the glycosidic conformations over the range  $190.9$ – $192.5$  pm. Examination of the interactions in the minima discloses the occurrence of an intramolecular hydrogen-bond between O-2' and O-3 in minima T5, T7, and T8 with oxygen–oxygen distances of  $258.9$ ,  $256.7$ , and  $257.1$  pm, respectively.

Interglycosidic proton–proton distances evaluated from n.m.r. experiments are often used as a probe of solution conformation. The calculated  $r_{14}$  and  $r_{13}$  distances presented in Table I illustrate the variability of these parameters with change of the conformation. They vary for stable conformers of **1** in a range between  $207.6$  and  $407.2$  pm for  $r_{14}$  and between  $199.5$  and  $519.4$  pm for  $r_{13}$ .



*Comparison with the crystal structures.* — A comparison of the calculated minima of **1** with the crystal structure<sup>2</sup> (Table I) showed that the minimum T15 at  $\Phi = 91.8^\circ$  and  $\Psi = -89.7^\circ$  is near to the crystal-structure conformation. The relative energy of this conformer is 17.5 kJ/mol. The calculated torsional angle  $\Phi$  of T15 fits nicely to its experimental counterpart  $\Phi = 89.1^\circ$ . The second torsional angle  $\Psi$  is shifted by  $27^\circ$  from the experimental value  $\Psi = -116.8^\circ$ . The calculated value of  $\tau = 101.5^\circ$  for the T15 conformer is in very good agreement with the experimental value  $\tau = 100.3^\circ$ .

The molecular packing of **1** shows<sup>2</sup> that all hydroxyl groups are involved in intermolecular hydrogen-bonds. As neither the influence of this hydrogen-bond pattern nor van der Waals forces in the crystal are taken into account by the present calculations, the small differences between the crystal structure of **1** and the calculated minimum T15 and the higher relative energy of T15 are understandable. Interestingly the crystal structure of heptyl 1-thio- $\alpha$ -D-glucopyranoside<sup>17</sup> is similar to the conformation of T4 and the experimental ( $112.0^\circ$ ) and calculated ( $112.4^\circ$ ) values of the O–C–S bond angle agree well.

The calculated values of C–S bond lengths are  $\sim 8$  pm larger than the experimental values. This feature seems to be characteristic of the PCILO method: similar values for the C–S bond lengths have been calculated for acyclic model compounds<sup>7</sup>. This is probably the result of ignoring the *d* orbitals on sulphur in this method. However, the computer modelling of the thioacetal segment is complicated, and results for model compounds showed<sup>7</sup> that the PCILO method correctly reproduces the energy of the conformers and the variations in bond angles and bond lengths.

There are six crystal structures of  $\alpha$ -(1 $\rightarrow$ 4)-O-linked disaccharides which may be considered as oxygen analogues of methyl 4-thio- $\alpha$ -maltoside. For this type of linkage, crystal structures may be divided into three groups, and the torsional angles  $\Phi$  and  $\Psi$  lie within the regions  $72.5$ – $121.7^\circ$  and  $-108.8^\circ$  to  $155.0^\circ$ , respectively. They are in the north part of the relaxed map for **1** where the T5, T7, T8, and T10 conformers are located. In contrast to the crystal structure of **1**, in  $\alpha$ -maltose<sup>18</sup>,  $\beta$ -maltose monohydrate<sup>19</sup>, methyl  $\beta$ -maltoside<sup>20</sup>, and phenyl  $\alpha$ -maltoside<sup>21</sup> intramolecular O-3H $\cdots$ O-2H hydrogen bonds occur and thus influence the conformations about the glycosidic linkage.

*Solvent-relaxed ( $\Phi$ ,  $\Psi$ ) maps.* — Fig. 4 shows the final solvent-specific relaxed ( $\Phi$ ,  $\Psi$ ) potential surface for **1** in four selected solvents, namely 1,4-dioxane, methanol, dimethyl sulfoxide, and water at  $25^\circ$ . Comparison of the maps in Fig. 4 shows variations as a result of solvent. A dominant effect is, in contrast to the observation found for the rigid map, a stabilization of the region having both  $\Phi$  and  $\Psi$  angles in the *sc* orientation (the south domain on the rigid map). There is a marked difference between the solvent effect of water and that of other solvents. It is noteworthy that the solvent effect of dimethyl sulfoxide is not as strong as expected on the basis of its dielectric constant. Similar solvent effects have been observed in our previous studies<sup>8,9</sup>.

The solvent effect also manifests itself in changes in the relative energies of the individual conformers. Molar fractions of the stable conformers estimated from calculated free-energy differences in the isolated state and in four solvents according to Eq. 1

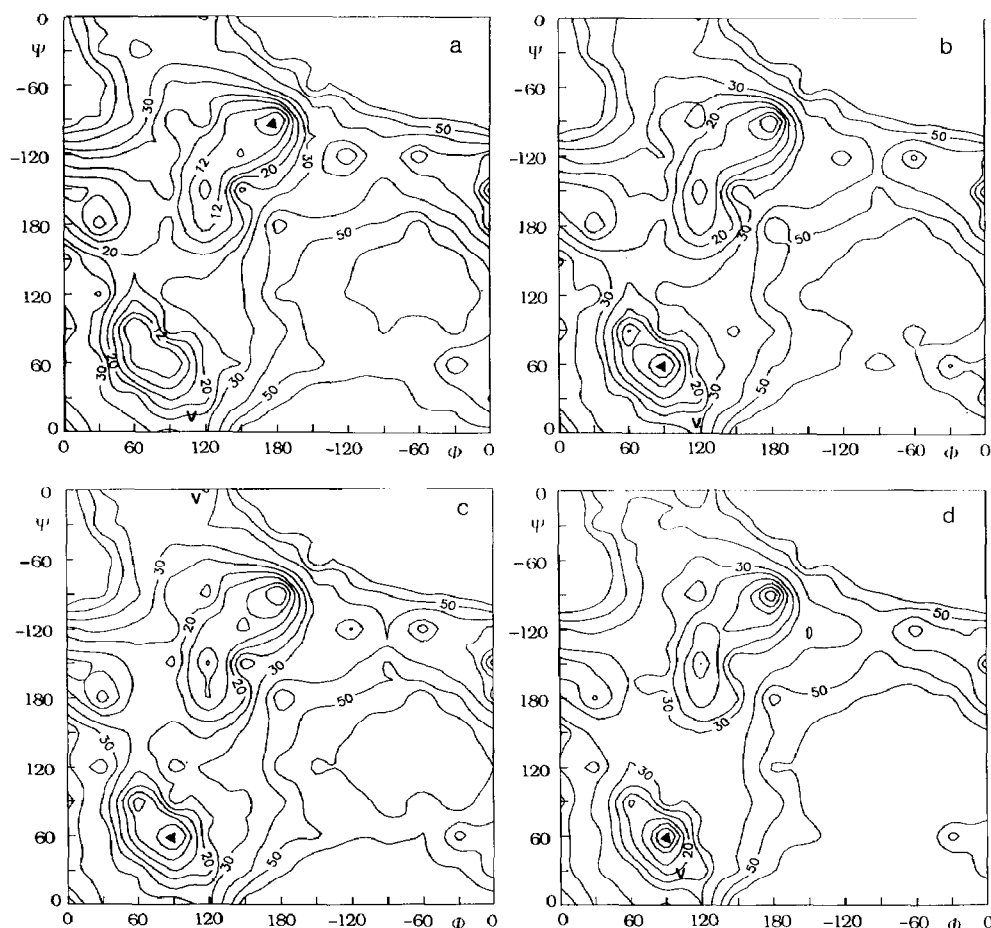


Fig. 4. Relaxed energy surface (kJ/mol) for methyl 4-thio- $\alpha$ -maltoside in four solvents [(a) 1,4-dioxane, (b) methanol, (c) dimethyl sulfoxide, and (d) water]. Contours are at 8, 12, 16, 20, 25, 30, 40, 50, and 60 kJ/mol around the energy minimum which is indicated by  $\blacktriangle$ . The "virtual" conformations are indicated by V on each map.

TABLE II

Calculated molar fractions of the stable conformers of methyl 4-thio- $\alpha$ -maltoside in a vacuum and solution

Conformation	Vacuum	1,4-Dioxane	Methanol	Dimethyl sulfoxide	Water
T1	44.1	28.9	3.1	6.9	0.2
T2	24.3	32.2	34.8	38.0	22.2
T3	13.0	23.9	57.8	48.3	76.6
T4	5.3	3.5	0.5	1.0	0.0
T5	3.6	3.9	2.1	2.8	0.7
T6	3.6	2.7	0.4	0.8	0.0
T7	2.4	1.7	0.3	0.5	0.0
T8	1.4	1.4	0.7	1.0	0.2
T9	1.1	0.8	0.2	0.3	0.0
T10	1.1	0.9	0.2	0.3	0.0

are given in Table II. The distribution of conformers for the isolated molecule is:  $T1 > T2 > T3 > T4 > T5 > T6 > T7 > T8 > T9 > T10$ . The energy of conformers T11–T15 is too high to be present in the equilibrium mixture. The results show that an increase of solvent polarity leads to a significantly lower abundance of the most stable conformer relative to the isolated molecule ( $T1 = 44.1\%$ ), that is, T1 is 3.1% in methanol and 0.2% in water. Analysis of the calculated data revealed that the dipole moment of this conformer is smaller compared to that for other conformers, especially T2 and T3, whereas the molecular volume is larger than in T2 and T3. Thus, electrostatic and cavity terms of solvation energy have a critical influence on the decrease of T1 conformers. The decrease of T1 with an increase of solvent polarity is counterbalanced by the increase of the T3 conformer, which lies in the same south domain (13% in vacuum, 76.6% in water). The net increase in the abundance of conformers occurring in this domain (T1, T3, and T6) is  $\sim 20\%$ . In 1,4-dioxane and dimethyl sulfoxide, however, the overall abundance of conformers in the south domain shows a small decrease (2–4%) while in methanol it increases (3%). Simultaneously, the abundance of the other conformers changes, with a larger variation observed for the T2 conformer. The abundance of this conformer increases from 24.3% in vacuum to 38% in dimethyl sulfoxide and then in water decreases to 22.2%, which is almost the same value as in a vacuum. The molecular drawings associated with the lowest conformation in vacuum and water are shown in Fig. 5.

The polarity of the solvent affects the distribution of hydroxymethyl-group conformers. For the torsional angle  $\omega_1$ , the stability of *gg* is dramatically increased from 51.0% in vacuum through 96.3% in methanol up to 99.7% in water. For the  $\omega_2$  angle, a solvent effect increases the abundance of the *tg* conformer, whereas abundances of the other two conformers are decreased. For example, the equilibrium *tg:gt:gg* at  $\omega_2$  varies from 22.7:44.8:27.4 in vacuum through 63.1:3.2:33.7 in methanol to 78.8:0.2:20.9 in water. Thus, in contrast to the observation that interactions with a solvent decrease the stability of the *tg* conformer found for glucopyranose<sup>22–24</sup>, this calculation shows that for  $\omega_2$  the *tg* conformer is the major species in water solution. A plausible explanation might be associated with the favourable interactions in the *tg* position of the hydroxymethyl group with the neighbouring residue.

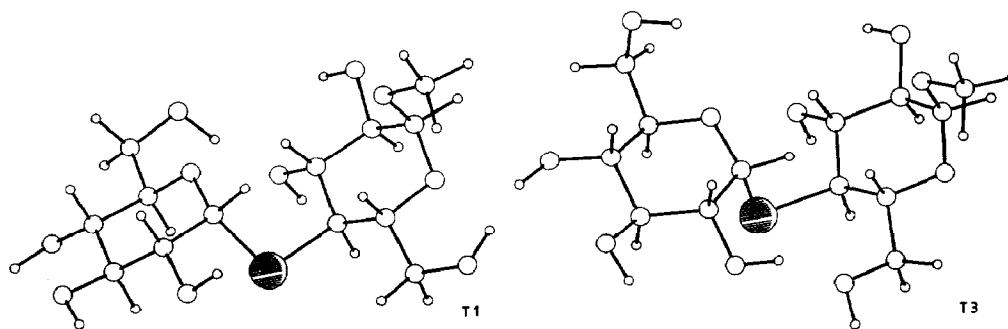


Fig. 5. Molecular depiction of the lowest energy conformation of methyl 4-thio- $\alpha$ -maltoside in a vacuum (T1) and water (T3).

*"Virtual" conformations.* — The present results show that methyl 4-thio- $\alpha$ -maltoside in solution undergoes internal motion and that the population of the molecule is distributed among several individual conformational states and is dependent on the solvent. This implies that experimentally observed parameters, such as, coupling constants, n.O.e. values, and  $T_1$  parameters measured by n.m.r. would be the result of averaging over all available conformational states during the time course of the experiment. The results derived from such experiments correspond, therefore, to the "virtual" conformations<sup>25</sup>. The importance of conformational averaging has been recently illustrated with methyl 3-*O*- $\alpha$ -D-mannopyranosyl- $\alpha$ -D-manopyranoside<sup>26</sup> where observed n.O.e. data were reproduced only when averaging over more than 500 conformational states. The calculated values of ensemble average geometrical parameters which describe the "virtual" conformation in different environmental situations at 25° are given in Table III and molecular drawings of the "virtual" conformation in vacuum and water are shown in Fig. 6. The values of ensemble average torsional angles  $\langle \Phi \rangle$  and  $\langle \Psi \rangle$  clearly demonstrate that the "virtual" conformation of methyl 4-thio- $\alpha$ -maltoside is sensitive to solvation. These virtual conformations do not correspond to any of the 15 calculated conformers of 1. In fact, they are located on the barrier hills (see Figs. 3 and 4), and thus in water this position is 25 kJ/mol above the global minimum T3. The same is true for the angle  $\langle \omega_1 \rangle$  ( $-8^\circ$ ) in vacuum and for the angle  $\langle \omega_2 \rangle$  in water ( $114^\circ$ ). The influence of solvent on  $\langle \mu \rangle$  is as expected: the magnitude of  $\langle \mu \rangle$  increases with polarity of the solvent. The values of the partition function given in Table III demonstrate a lower flexibility of 1 in water ( $Q = 2.5$ ) relative to a vacuum ( $Q = 4.3$ ) and especially to 1,4-dioxane ( $Q = 5.9$ ).

TABLE III

Ensemble averages of the selected dihedral angles ( $\Phi$ ,  $\Psi$ ,  $\omega_1$ ,  $\omega_2$ ), bond angles ( $\alpha$ ,  $\tau$ ), partition function ( $Q$ ), dipole moment ( $\mu$ ), proton-proton distances,  $r_{ij}$ ,  $r_{ij}^{-6} \times 10^{12}$  and carbon-proton coupling constant  $^3J_{C,H}$  in solution

	Vacuum	1,4-Dioxane	Methanol	Dimethyl sulfoxide	Water
$\langle \Phi \rangle$	95.8	108.3	119.4	121.0	109.0
$\langle \Psi \rangle$	25.7	9.0	4.5	-1.6	26.6
$\langle \omega_1 \rangle$	-8.2	-23.9	-51.4	-47.2	-54.5
$\langle \omega_2 \rangle$	45.7	47.8	79.7	66.3	113.9
$\langle Q \rangle$	4.3	5.9	3.3	3.9	2.5
$\langle \mu \rangle$	4.5	5.3	6.9	6.6	7.3
$\langle r_{12} \rangle$	456.58	458.88	459.31	459.84	458.07
$\langle r_{12}^{-6} \rangle$	0.0001	0.0001	0.0001	0.0001	0.0001
$\langle r_{13} \rangle$	240.32	254.54	255.25	262.20	231.39
$\langle r_{13}^{-6} \rangle$	0.0243	0.0190	0.0126	0.0128	0.0144
$\langle r_{14} \rangle$	333.56	324.76	325.29	320.76	339.96
$\langle r_{14}^{-6} \rangle$	0.0022	0.0023	0.0018	0.0021	0.0011
$\langle r_{15} \rangle$	278.64	278.09	260.10	267.61	242.70
$\langle r_{15}^{-6} \rangle$	0.0045	0.0045	0.0056	0.0051	0.0069
$\langle ^3J_{C-4,H-1'} \rangle$	1.54	1.71	2.28	2.10	2.67
$\langle ^3J_{C-1',H-4} \rangle$	4.23	4.25	4.73	4.52	5.24

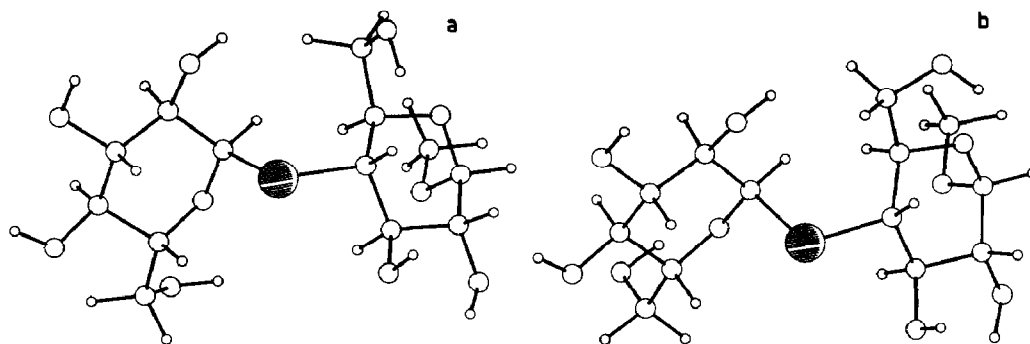


Fig. 6. Molecular depiction of the shape of the "virtual" conformation in a vacuum (a) and water (b).

The calculated  $\langle {}^3J_{C,H} \rangle$  values nicely reflect differences in conformational surface with the solvent. The  $\langle {}^3J_{C4,H-1'} \rangle$  value increases from 1.54 Hz in vacuum to 2.67 Hz in water. A similar change from 4.23 to 5.24 Hz is predicted for the  $\langle {}^3J_{C-1',H-4'} \rangle$  value. The difference of 1 Hz in both  $\langle {}^3J_{C,H} \rangle$  values show how useful these coupling constants can be for investigation of conformational properties of oligosaccharides. This is not surprising, since the  ${}^3J_{C,H}$  values change rapidly with torsional angle and so a slight change in the distribution of torsional angle may change the coupling constant considerably.

An ensemble average of the inverse sixth power of the interglycosidic proton-proton distances  $\langle r_{ij}^{-6} \rangle$  show how differently sensitive can various n.o.e. and  $T_1$  values be to the change of the internal flexibility about glycosidic linkages of **1** imposed by a solvent. Although interglycosidic proton-proton distances  $r_{ij}$  vary significantly from conformer to conformer (Table I), the  $\langle r_{14}^{-6} \rangle$  and  $\langle r_{12}^{-6} \rangle$  values are fairly constant and suggest that these distances do not sufficiently reflect internal motions of **1**. A larger variation is observed for distance between the protons H-1' and H-3. It has been shown<sup>27</sup> that, because of the resulting strong dependence of the ensemble average on the inverse proton-proton distance, only those conformations corresponding to small values of  $r_{ij}$  contribute significantly to the average, regardless of the dependence of the weighting factor  $x_i$  on conformation. Therefore, we have investigated which conformers of **1** contribute to  $\langle r_{ij}^{-6} \rangle$ . Close inspection of contributions to the ensemble averages of  $\langle r_{ij}^{-6} \rangle$  from different conformations of the relaxed  $(\Phi, \Psi)$  maps revealed an important role of conformers having short proton-proton distances. For example, for the H-1'-H-4 distance, the three largest contributions to  $\langle r_{14}^{-6} \rangle$  in vacuum come from conformers T6, T10, and T5, which have relative energies 6.2, 1.5, and 7.4 kJ/mol, respectively. Similarly for H-1'-H-3, the three largest contributions to  $\langle r_{13}^{-6} \rangle$  in vacuum are from the T6, T1, and T3 conformers, which have the relative energies 0.0, 0.1, and 3.1 kJ/mol. In water solution, the conformers T3, T1, and T6 with the energies of 0.0, 14.7, and 14.6 kJ/mol are the largest contributors. Significant contributions to  $\langle r_{ij}^{-6} \rangle$  from conformers having high relative energies complicates an application of these parameters for the determination of solution conformations of **1**, especially when the accuracy<sup>28</sup> of the  $r_{ij}$  value estimated from n.m.r. data is  $\sim 20$  pm. In addition, the  $\langle r_{ij}^{-6} \rangle$  data in Table III

indicate that the same theoretical n.O.e. or  $T_1$  values may be derived that are in reasonable agreement with experimental data from very different potential surfaces.

*Comparison with solution properties.* — The proposed angular dependence of the vicinal carbon–proton coupling constant  $^3J_{C,H}$  for C–S–C–H segment of atoms makes it possible to calculate theoretical  $\langle ^3J_{C,H} \rangle$  values and compared them with observed values  $^3J_{C-4,H-1'} = 2.95$  Hz and  $^3J_{C-1',H-4} = 5.15$  Hz in water solution<sup>3</sup>. These values differ considerably from the values  $^3J_{C-4,H-1'} = 3.1$  Hz and  $^3J_{C-1',H-4} = 3.8$  Hz calculated for the crystal-structure conformation of **1** using torsional angles  $\Phi^H = -25.6^\circ$  and  $\Psi^H = 3.6^\circ$ . This observation shows, as expected from our results, that methyl 4-thio- $\alpha$ -maltoside in water solution can not be described adequately either by crystal structure conformation or by the T3 (77 %) which is the dominant conformer in water solution. For this conformer having  $\Phi^H = -22.9^\circ$  and  $\Psi^H = 176.3^\circ$ , the  $^3J_{C-4,H-1'} = 3.24$  Hz and  $^3J_{C-1',H-4} = 5.93$  Hz values were calculated. Similarly, the calculated  $\langle ^3J_{C,H} \rangle$  values from the vacuum-relaxed map differ significantly from the measured values. In contrast to vacuum, the ensemble average  $\langle ^3J_{C,H} \rangle$  values calculated for water solution, 2.67 and 5.24 Hz (Table III), are in very good agreement with experimental values. This concordance suggests that the calculated relaxed surfaces correctly describe the solution behaviour of **1**. Further data that support this conclusion are the calculated  $\langle ^3J_{C,H} \rangle$  values 2.6 and 5.2 Hz, based only on the equilibrium of five stable conformers. Thus, it is also very likely that the calculated conformers correctly represent the conformational equilibrium of **1** in solution. This clearly implies that, for the adequate description of the conformational equilibrium of **1** in solution, it is necessary to incorporate the solvent effect into the calculation of the relaxed map.

## CONCLUSIONS

The present calculations of the PCILO relaxed maps for methyl 4-thio- $\alpha$ -maltoside clearly demonstrate the flexibility of this molecule. A comparison of the solvent-specific relaxed maps shows that conformational properties are strongly influenced by solvent. This is demonstrated by the different geometries of the global minima in different solvents and by variations in the “virtual” conformation structures. Notably, a flexibility of methyl 4-thio- $\alpha$ -maltoside about the glycosidic torsional angles is strongly decreased in water solution in comparison with other solvents. Despite the inherent limitations in the calculation of solvent effects, we conclude that inclusion of solvation effects is required for the reliable representation of conformational behaviour of oligosaccharides in solution. An additional aspect of the present work has been a comparison of the conformational properties of methyl 4-thio- $\alpha$ -maltoside with its oxygen analogue maltose. While the vacuum-rigid maps of both compounds are similar, the vacuum-relaxed maps and the solution behaviour of both molecules differ considerably. The very good agreement between calculated and experimental  $\langle ^3J_{C,H} \rangle$  values suggest that conformational properties and solution behaviour of methyl 4-thio- $\alpha$ -maltoside are adequately predicted by the present calculations.

## ACKNOWLEDGMENT

A grant for supporting the sabbatical stay of one of us (I.T.) in CERMAV, Grenoble was supplied by the Centre National de la Recherche Scientifique.

## REFERENCES

- 1 M. Blanc-Muesser, J. Defaye, H. Driguez, and E. Ohleyer, in W. Palz, P. Chartier and D. O. Hall (Eds.), *Energy from Biomass*, Applied Science, London, 1981, pp. 312–318.
- 2 S. Pérez and C. Vergelati, *Acta Crystallogr., Sect. B*, 40 (1984) 294–299.
- 3 I. Tvaroska, K. Mazcau, M. Blanc-Muesser, S. Lavaitte, H. Driguez, and F. R. Taravel, *Carbohydr. Res.*, submitted.
- 4 I. Tvaroska, *Collect. Czech. Chem. Commun.*, 49 (1984) 345–354.
- 5 A. D. French and J. W. Brady (Eds.), *Computer Modeling of Carbohydrate Molecules*, ACS Symp. Ser., 430 (1989).
- 6 S. Diner, J. P. Malrieu, F. Jordan, and M. Gilbert, *Theoret. Chim. Acta*, 15 (1969) 100–110.
- 7 I. Tvaroska and T. Bleha, *Adv. Carbohydr. Chem. Biochem.*, 47 (1989) 45–123.
- 8 I. Tvaroska and T. Kozar, *J. Am. Chem. Soc.*, 102 (1980) 6929–6936.
- 9 I. Tvaroska, *Biopolymers*, 21 (1982) 1887–1897.
- 10 I. Tvaroska, *Pure Appl. Chem.*, 61 (1989) 1201–1216.
- 11 I. Tvaroska and S. Pérez, *Carbohydr. Res.*, 149 (1986) 389–410.
- 12 M. J. D. Powell, *Comput. J.*, 7 (1964) 155–162.
- 13 W. I. Zangwill, *Comput. J.*, 10 (1967) 293–296.
- 14 I. Tvaroska, *Biopolymers*, 21 (1982) 1887–1897.
- 15 V. Tran, A. Buléon, A. Imberty, and S. Pérez, *Biopolymers*, 28 (1989) 679–690.
- 16 S. N. Ha, L. J. Madsen, and J. W. Brady, *Biopolymers*, 27 (1988) 1927–1952.
- 17 H. A. van Doren, R. van der Geest, F. van Bolhuis, R. M. Kellogg, and H. Wynberg, *Carbohydr. Res.*, 194 (1989) 79–86.
- 18 F. Takusagawa and R. A. Jacobson, *Acta Crystallogr., Sect. B*, 34 (1978) 213–218.
- 19 M. E. Gress and G. A. Jeffrey, *Acta Crystallogr., Sect. B*, 33 (1977) 2490–2495.
- 20 S. S. Chu and G. A. Jeffrey, *Acta Crystallogr.*, 23 (1967) 1038–1049.
- 21 I. Tanaka, N. Tanaka, T. Ashida, and M. Kakuda, *Acta Crystallogr., Sect. B*, 32 (1976) 155–160.
- 22 I. Tvaroska and T. Kozar, *Theor. Chim. Acta*, 70 (1986) 99–114.
- 23 L. M. Kroon-Batenburg and J. Kroon, *Biopolymers*, 29 (1990) 1243–1248.
- 24 S. Ha, J. Gao, B. Tidor, J. W. Brady, and M. Karplus, *J. Am. Chem. Soc.*, 113 (1991) 1553–1557.
- 25 O. Jardetzky, *Biochim. Biophys. Acta*, 621 (1980) 227–232.
- 26 A. Imberty, V. Tran, and S. Pérez, *J. Comput. Chem.*, 11 (1989) 205–216.
- 27 D. A. Brant and M. D. Christ, *ACS Symp. Ser.*, 430 (1990) 42–68.
- 28 P. Daïs and A. S. Perlin, *Adv. Carbohydr. Chem. Biochem.*, 45 (1987) 125–168.